

Supporting Information

Melt Viscosity Behavior of C₆₀ Containing Star Polystyrene composites

Haiying Tan,^{a,b} Donghua Xu,^a Dong Wan,^{a,b} Yujie Wang,^{a,b} Lu Wang,^{a,b} Jun Zheng,^{a,b} Feng Liu,^{a,b}

*Li Ma,^a and Tao Tang ^{*a}*

^a *State Key Laboratory of Polymer Physics and Chemistry, Changchun Institute of Applied Chemistry,*

Chinese Academy of Sciences, Changchun 130022, China

^b *Graduate School of the Chinese Academy of Sciences, Beijing 100039, China*

* To whom correspondence should be addressed.

Tel: +86 (0) 431 85262004

Fax: +86 (0) 431 85262827

E-mail: ttang@ciac.jl.cn

Table of Content

Figure or Table	Page Number	Content
	3	Continuous Relaxation Spectra
Table S1	3	Summary of $\eta_{0.05}^*$, G_N^0 , η_a and T_g for LPS-22k, LPS-212k and their blends with C_{60} .
Table S2	4	Summary of η_0 , G_N^0 , η_a and τ_a for pure SPSs and their blends with C_{60} .
Figure S1	4	^1H NMR spectra of the synthesized polystyrene
Figure S2	5	TEM images of S3PS-48k-5 and S3PS-119k-5
Figure S3	5	SAXS profiles of S3PS-75k-1 composites before and after rheology
Figure S4	6	The changing trend of G' and G'' of S3PS-48k/ C_{60} composites
Figure S5	7	The changing trend of η^* , G' and G'' of S3PS-75k/ C_{60} composites
Figure S6	8	The changing trend of G' and G'' of S3PS-119k/ C_{60} composites
Figure S7	9	The changing trend of η^* , G' and G'' of S3PS-150k/ C_{60} composites
Figure S8	10	The changing trend of G' and G'' of S6PS-93k/ C_{60} composites
Figure S9	11	The changing trend of η^* , G' and G'' of S6PS-226k/ C_{60} composites
Figure S10	12	The changing trend of G' and G'' of LPS/ C_{60} composites
Figure S11	13	η_0 , η_a , $\eta_{0.05}^*$, τ_a and G_N^0 of S3PS-48k/ C_{60} composites versus the concentration of C_{60}
Figure S12	14	η_0 , η_a , $\eta_{0.05}^*$, τ_a and G_N^0 of S3PS-75k/ C_{60} composites versus the concentration of C_{60}
Figure S13	15	η_0 , η_a , $\eta_{0.05}^*$, τ_a and G_N^0 of S6PS-93k/ C_{60} composites versus the concentration of C_{60}
Figure S14	16	η_0 , η_a , $\eta_{0.05}^*$, τ_a and G_N^0 of S3PS-119k/ C_{60} composites versus the concentration of C_{60}
Figure S15	17	η_0 , η_a , $\eta_{0.05}^*$, τ_a and G_N^0 of S3PS-150k/ C_{60} composites versus the concentration of C_{60}
Figure S16	18	η_0 , η_a , $\eta_{0.05}^*$, τ_a and G_N^0 of S6PS-226k/ C_{60} composites versus the concentration of C_{60}
Figure S17	19	Master curve of S3PS-48/150k blend at 150 °C.
Figure S18	19	The changing trend of η^* , G' and G'' of S3PS-48/S3PS-150k blends
Figure S19	19	Comparison of η^* , G' and G'' obtained at different gaps.
Figure S20	20	Elution curves of S3PS-48k from SEC measurement

Figure S21 20 Figure showed how the zero shear viscosity determined.

Continuous Relaxation Spectra.

The TRIOS software available with the ARES-G2 rheometer was used to evaluate the continuous relaxation spectra, using both the G' (storage modulus) and G'' (loss modulus) data. The continuous relaxation time spectrum can be extracted by fitting following model with n terms to either oscillation ($G'(w)$, $G''(w)$) or Relaxation ($G(t)$) data.

$$d \ln \tau = \frac{d\tau}{\tau}, g(\tau)\tau = H(\ln \tau)$$

$$G(t) = G_e + \int_{-\infty}^{+\infty} H(\ln \tau) e^{-t/\tau} d \ln \tau$$

$$G' = \int_{-\infty}^{+\infty} H(\ln \tau) \frac{\omega^2 \tau^2}{1 + \omega^2 \tau^2} d \ln \tau$$

$$G'' = \int_{-\infty}^{+\infty} H(\ln \tau) \frac{\omega \tau}{1 + \omega^2 \tau^2} d \ln \tau$$

For the numerical computation the spectrum $H(\ln\tau)$ is discretized (typical in the order of 100 steps). The spectrum represents all the pairs of fitted $\{H_i, \tau_i\}$ parameters and can be extracted into a new file if desired.

Table S1. Zero shear viscosity (η_0), plateau modulus (G_N^0), apparent relaxation time (τ_a) and glass transition temperature (T_g) for LPS-22k, LPS-212k and their blends with C₆₀.

Sample	τ_a (s)	T_g (°C)	G_N^0 (Pa)	$\eta_{0.05}^*$ (Pa*s)
LPS-22k	0.177	103.80	175121	35264
LPS-22k-1	0.191	103.60	172178	39275
LPS-212k	18.743	105.20	142804	930844
LPS-212k-1	18.554	104.90	123549	818497

(Zero shear viscosity was determined from the complex viscosity at the low frequency (0.05 rad/s) at the measured regime.)

Table S2 Zero shear viscosity (η_0), plateau modulus (G_N^0), apparent viscosity (η_a) and apparent relaxation time (τ_a) for pure SPSs and their blends with C_{60} .

Sample	τ_a (s)	G_N^0 (Pa)	η_0 (Pa · s) ^a × 10 ³	η_a (Pa · s)
S3PS-48k	0.045	223273	35.5±3.8	10047.3
S3PS-48k-1	0.035	202237	15.7±1.3	7078.3
S3PS-48k-5	0.062	220234	36.0±3.2	13654.5
S3PS-75k	0.242	171028	55.9±3.7	41388.8
S3PS-75k-1	0.191	164881	41.5±2.9	31492.2
S3PS-75k-5	0.215	191593	52.1±2.6	41192.5
S3PS-119k	0.842	145707	129.9±4.5	122685.3
S3PS-119k-1	0.944	158969	144.5±3.9	150066.7
S3PS-119k-2	1.052	164481	160.9±6.5	173034.0
S3PS-119k-5	1.996	161162	240.1±6.2	321679.4
S3PS-150k	1.248	148312	166.5±3.4	185093.4
S3PS-150k-1	2.182	157131	260.7±5.2	342859.8
S3PS-150k-2	2.863	142146	290.5±6.3	406964.0
S3PS-150k-5	2.591	154389	296.4±5.8	400021.9
S6PS-93k	0.070	209537	40.6±2.5	14667.6
S6PS-93k-1	0.057	200107	27.9±1.1	11406.1
S6PS-93k-5	0.078	278548	45.0±2.2	21726.7
S6PS-226k	1.338	157244	182.8±3.8	210392.5
S6PS-226k-1	1.448	150599	191.3±1.6	218067.4
S6PS-226k-5	1.459	151645	199.2±2.2	221250.1

^a Steady shear rheology was performed at the shear rate from 10^{-3} to 10 s⁻¹. Zero shear viscosity (η_0) was determined from the steady shear viscosity at the low shear rate, as shown in Figure S19

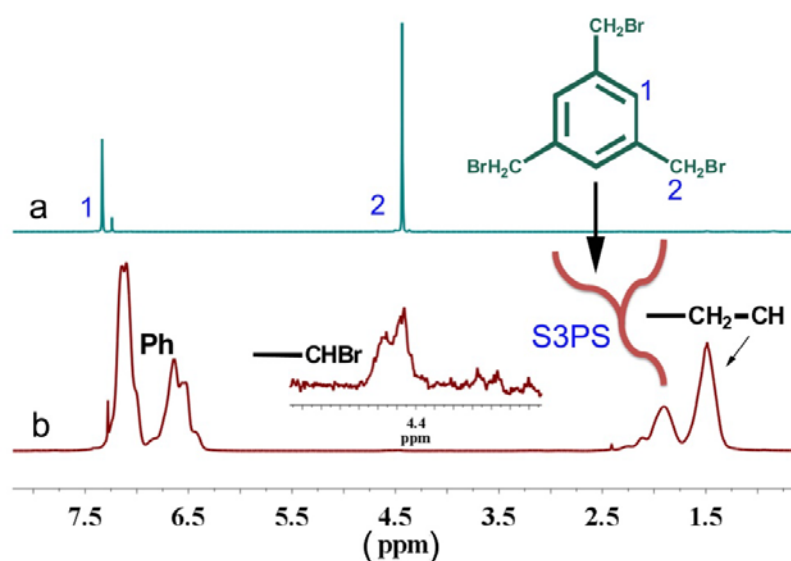


Figure S1. ¹H NMR spectra of (a) ATRP initiator and (b) S3PS.

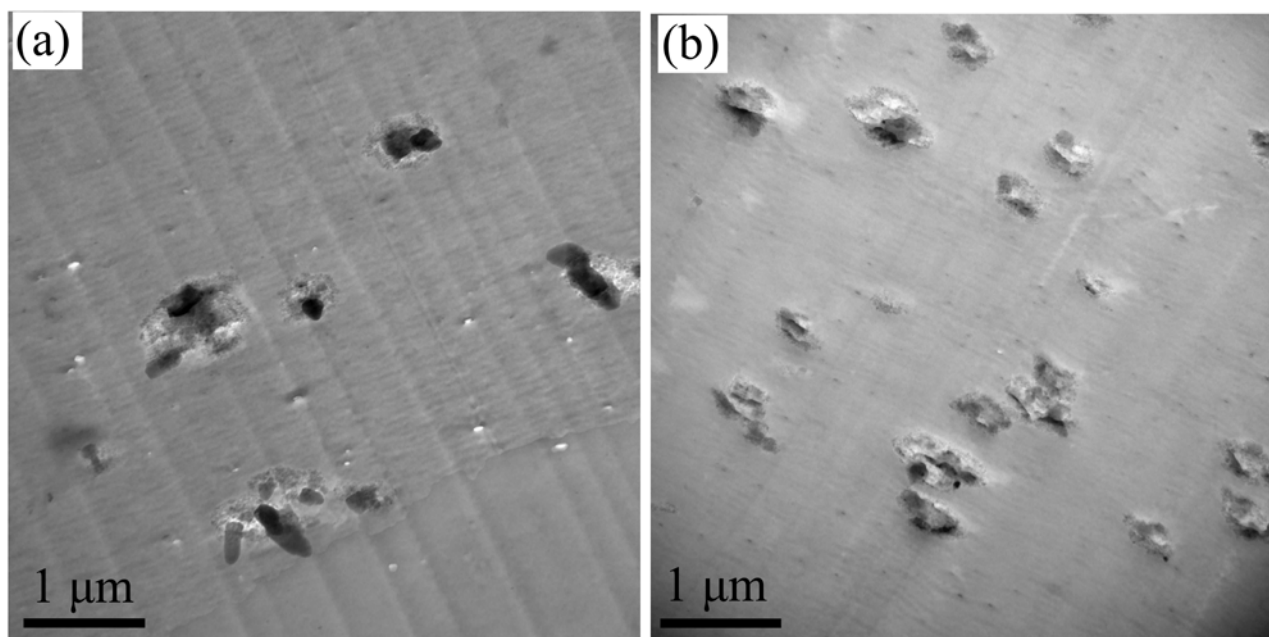


Figure S2. TEM images of (a) S3PS-48k with 5 wt% C₆₀ (S3PS-48k-5) and (b) S3PS-119k with 5 wt% C₆₀ (S3PS-119k-5)

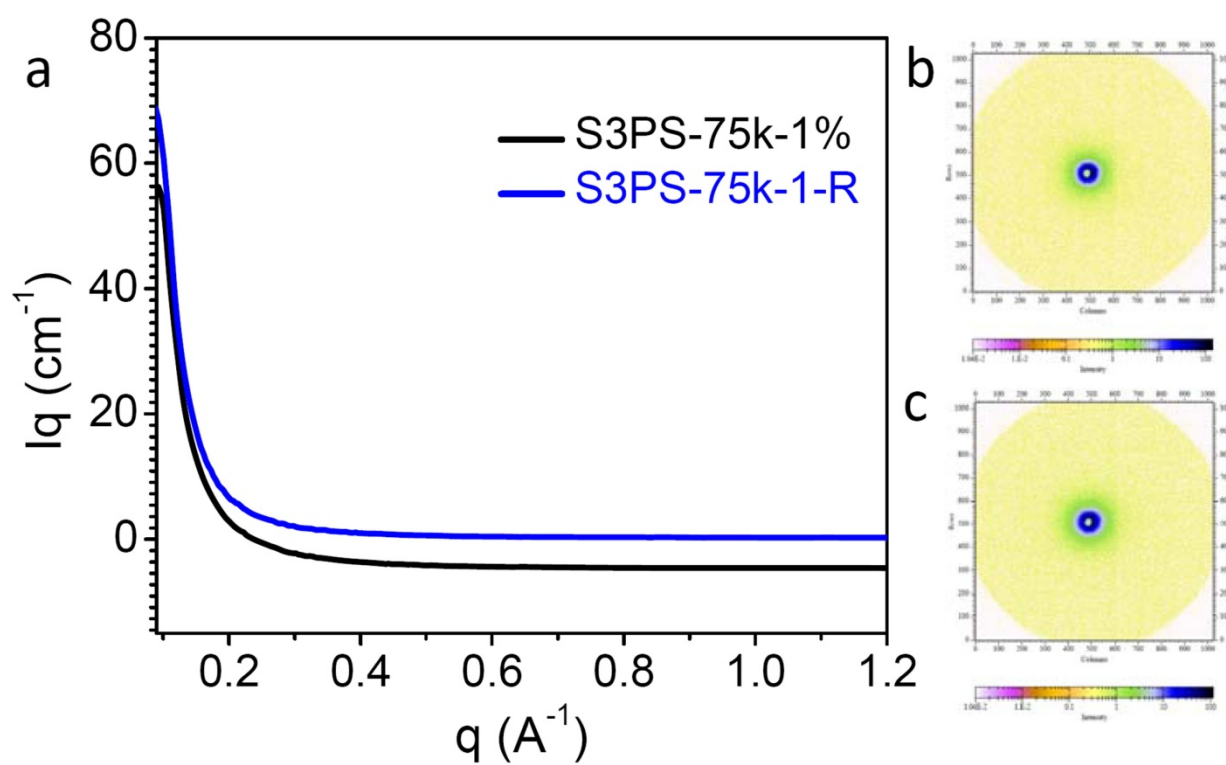


Figure S3. (a) SAXS results of S3PS-75k-1 before and after rheological measurements; (b) 2D SAXS image of S3PS-75k-1 before rheological measurements; (c) 2D SAXS image of S3PS-75k-1 after rheological measurements. The symbol 'R' represents the sample suffering rheological test.

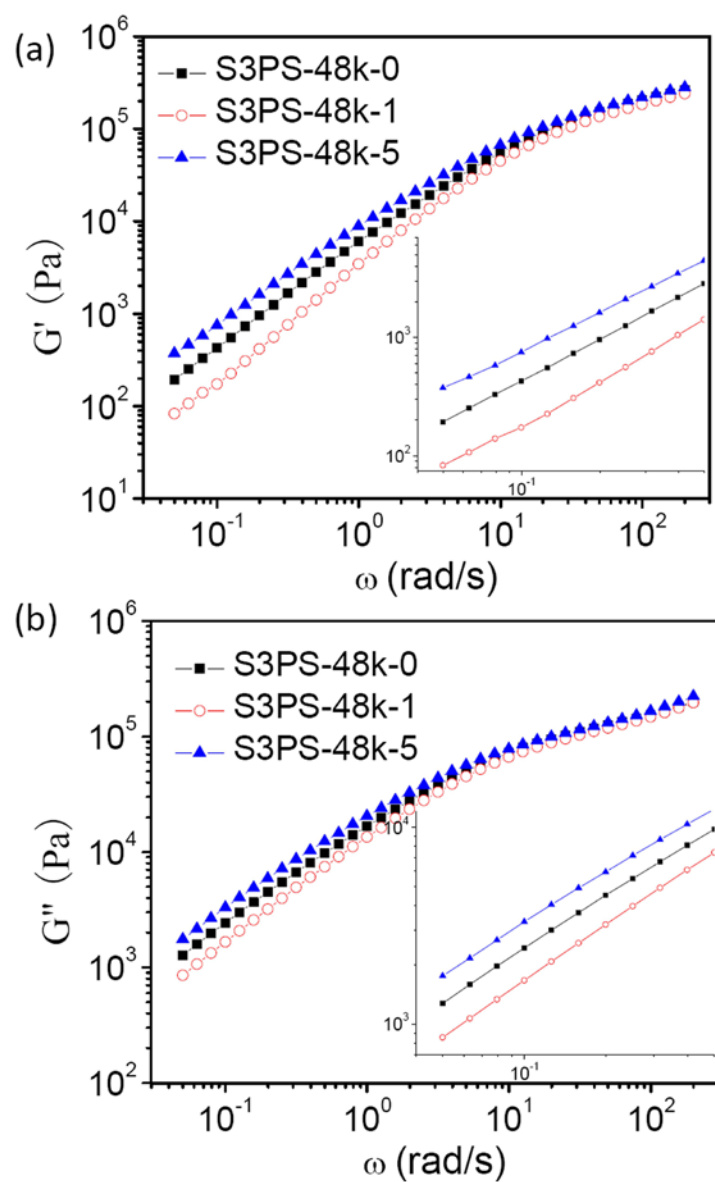


Figure S4. Storage modulus (G') (a) and loss modulus (G'') (b) versus frequency (ω) for S3PS-48k with different content of C_{60} . (Testing temperature: 150 °C).

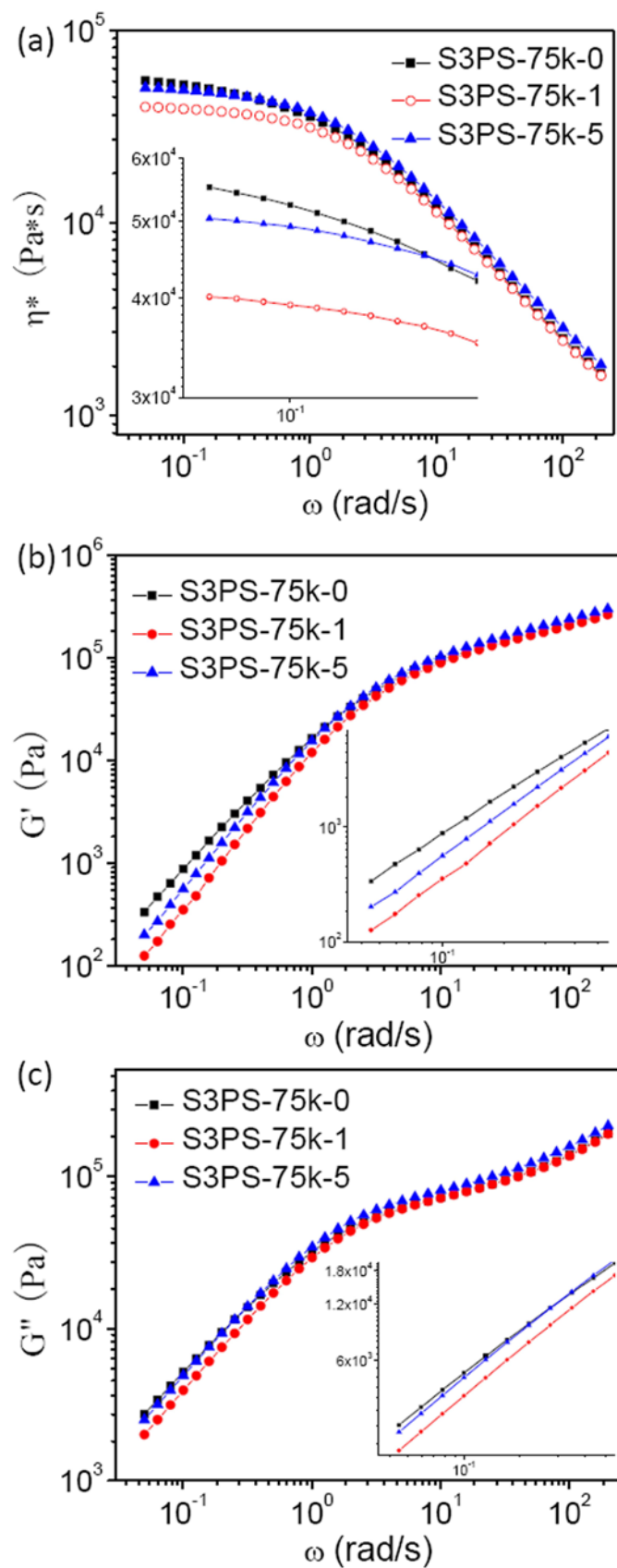


Figure S5. Complex viscosity (η^*) (a), storage modulus (G') (b) and loss modulus (G'') (c) versus frequency (ω) for S3PS-75k with different content of C_{60} . (Testing temperature: 150 °C).

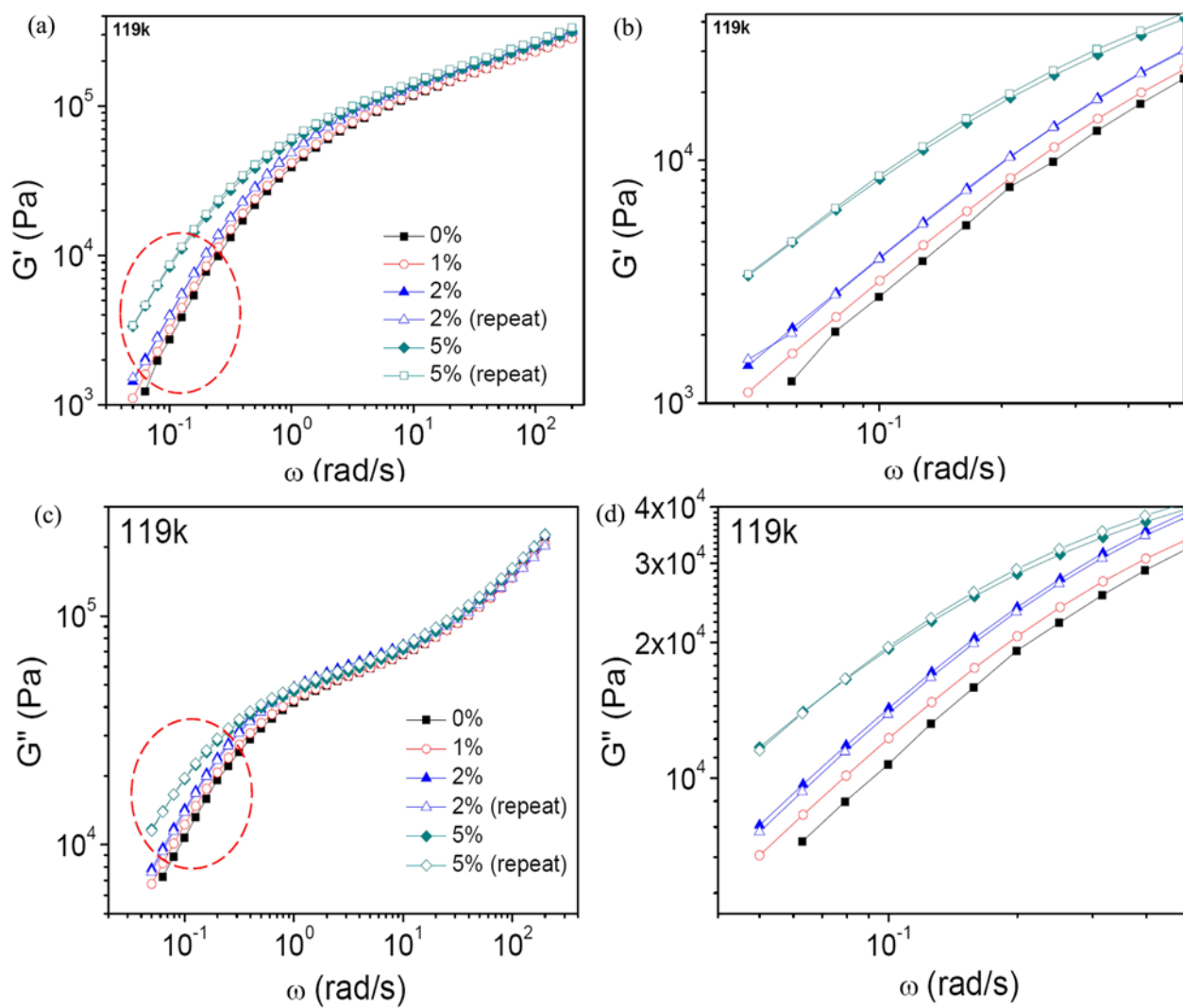


Figure S6. Storage modulus (G') (a) and loss modulus (G'') (b) versus frequency (ω) for S3PS-119k with different content of C₆₀. (Testing temperature: 150 °C). The symbol “repeat” in the figure represent the data of the samples were measured repeatedly. (b) and (d) were the zoom in of (a) and (b), respectively.

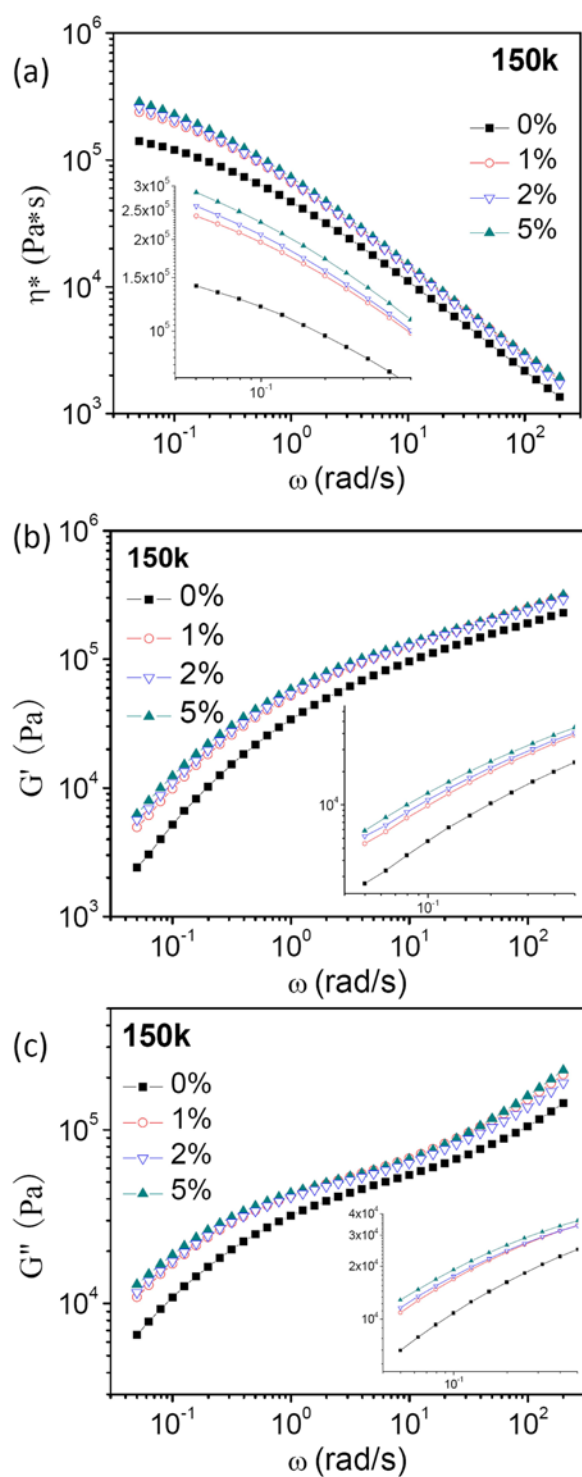


Figure S7. Complex viscosity (η^*) (a), storage modulus (G') (b) and loss modulus (G'') (c) versus frequency (ω) for S3PS-150k with different content of C₆₀. (Testing temperature: 150 °C).

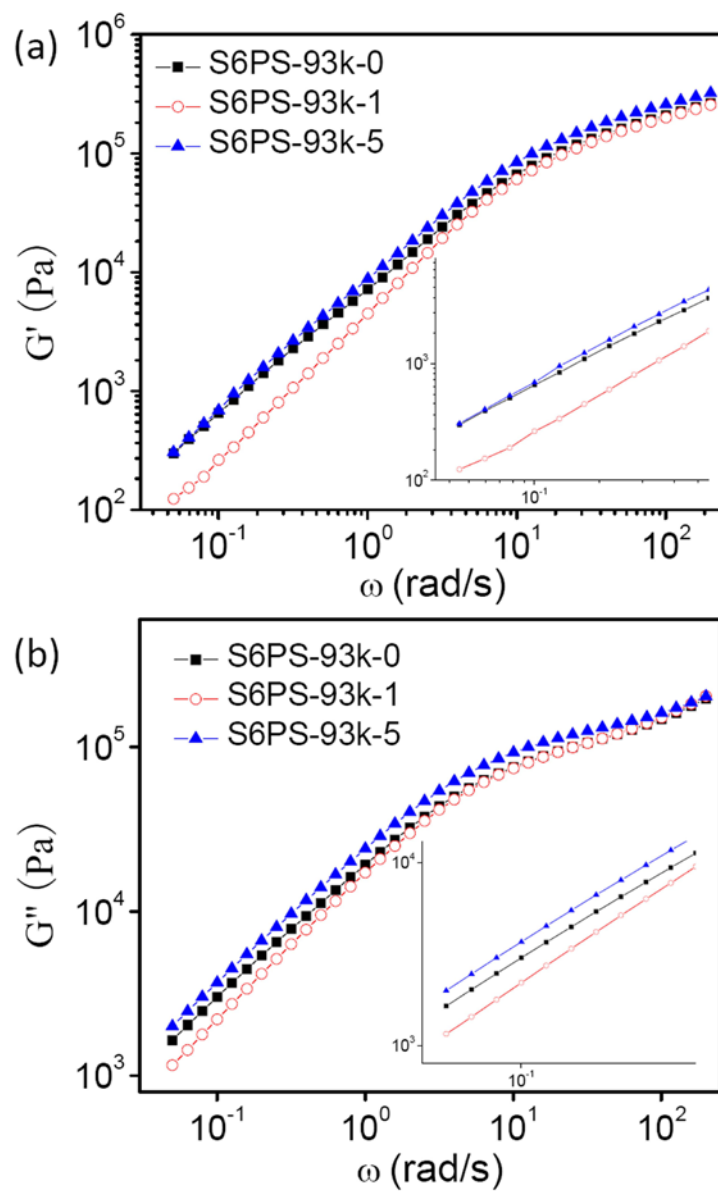


Figure S8. Storage (G') and loss (G'') moduli versus frequency (ω) for S6PS with different content of C_{60} for S6PS-93k (Testing temperature: 150 °C).

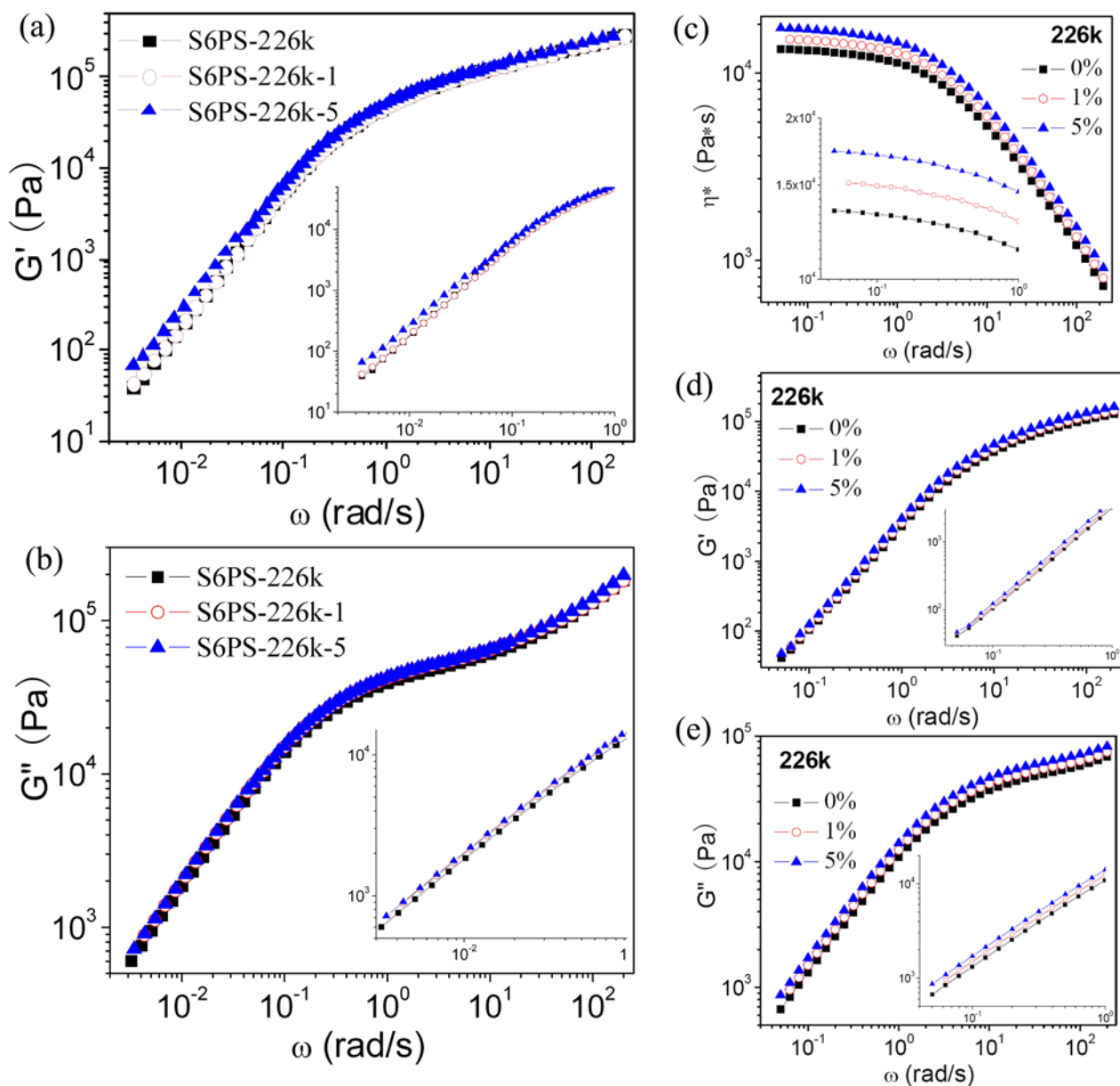


Figure S9. Complex viscosity (η^*) (at 170 °C), storage (G') and loss (G'') moduli versus frequency (ω) for S6PS with different content of C₆₀ for S6PS-226k. The data on the left side (a and b) and on the right side (c, d and e) was measured at 150 °C and 170 °C, respectively.

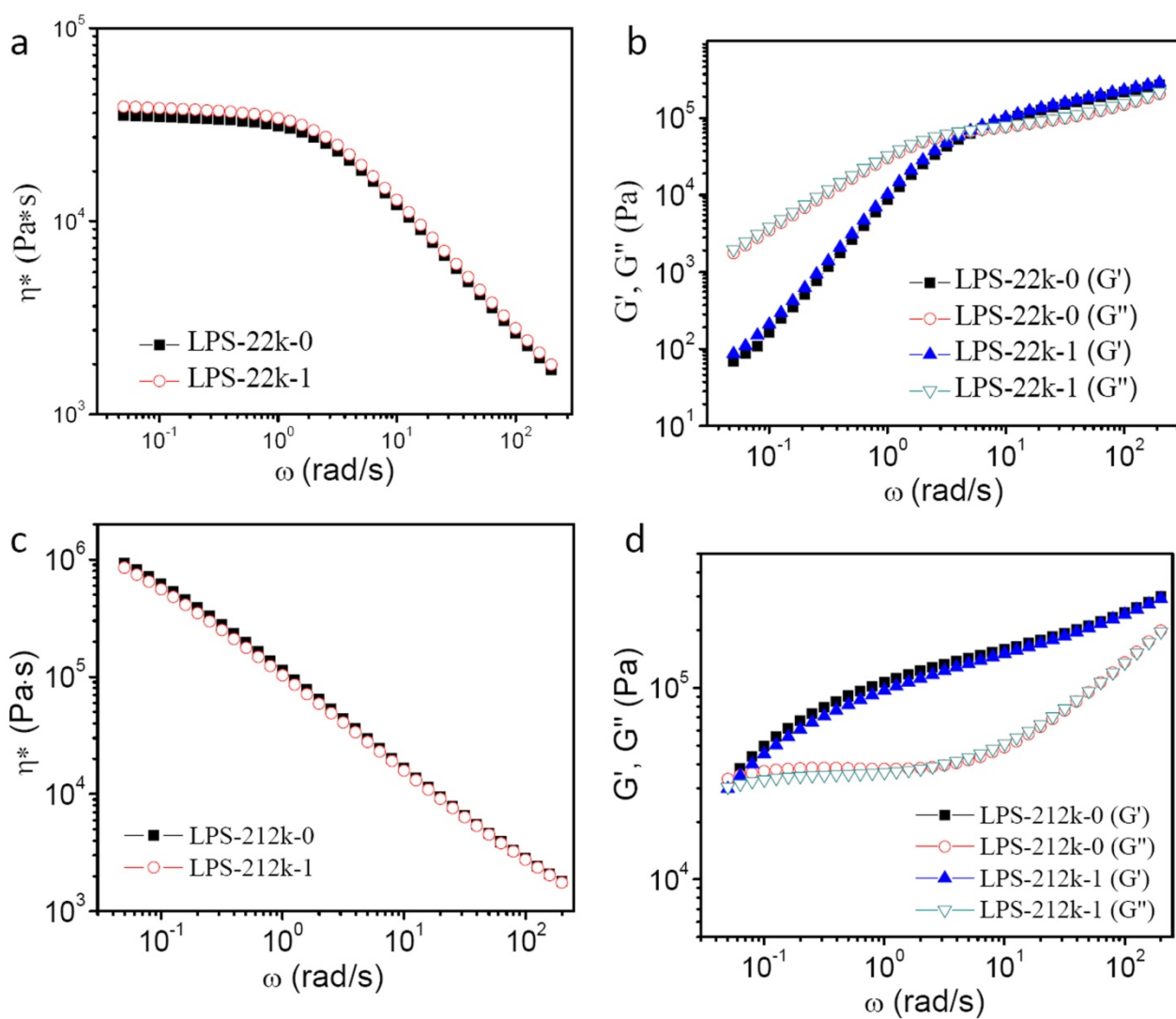


Figure S10. Complex viscosity (η^*), storage (G') and loss (G'') moduli versus frequency (ω) for LPS with different content of C_{60} . (a) and (b) for LPS-22k (unentangled), and (c) and (d) for LPS-212k (entangled) (b) (Testing temperature: 150 °C).

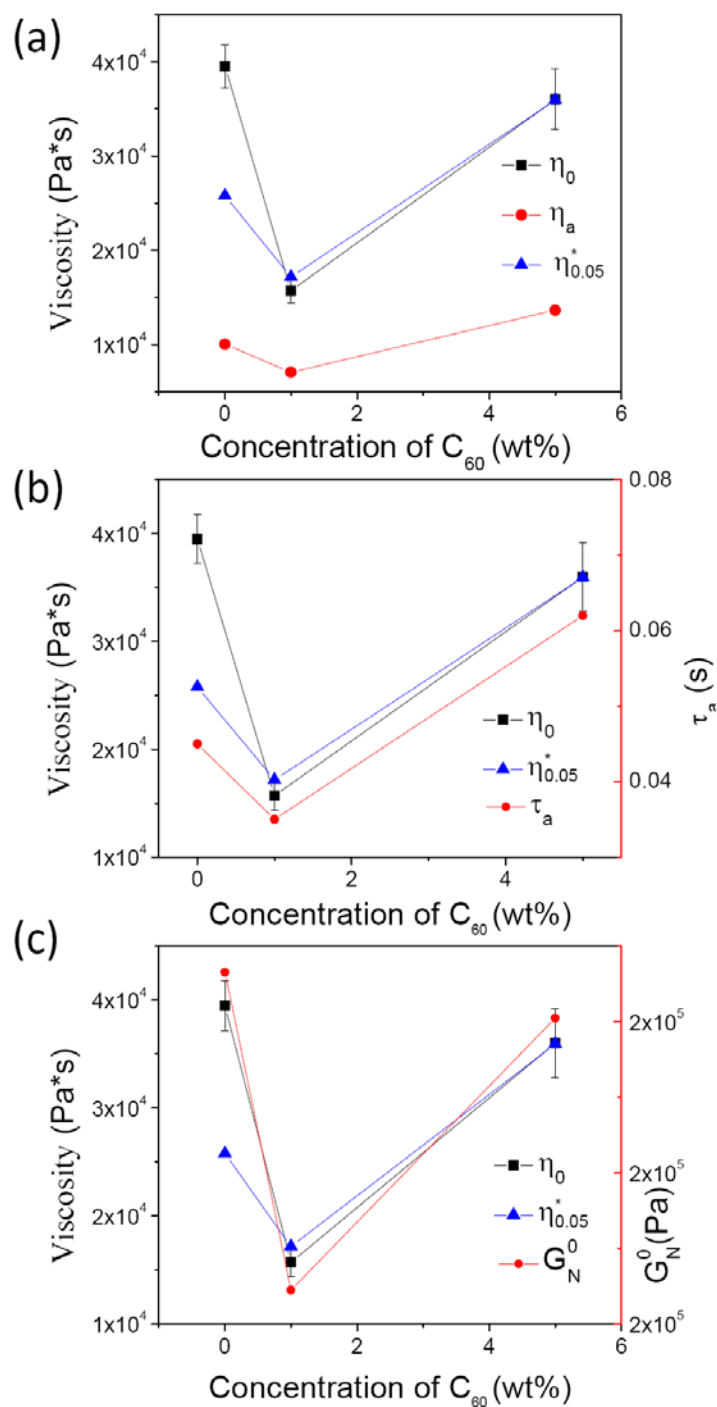


Figure S11. (a) Zero shear viscosity (η_0), complex viscosity at 0.05 rad/s ($\eta_{0.05}^*$) and apparent viscosity ($\eta_a = G_N^0 \cdot \tau_a$) of S3PS-48k/C₆₀ composites versus the concentration of C₆₀; (b) η_0 , $\eta_{0.05}^*$ and apparent relaxation time (τ_a) of S3PS-48k/C₆₀ composites versus the concentration of C₆₀; (c) η_0 , $\eta_{0.05}^*$ and plateau modulus (G_N^0) of S3PS-48k/C₆₀ composites versus the concentration of C₆₀ (Testing temperature: 150 °C).

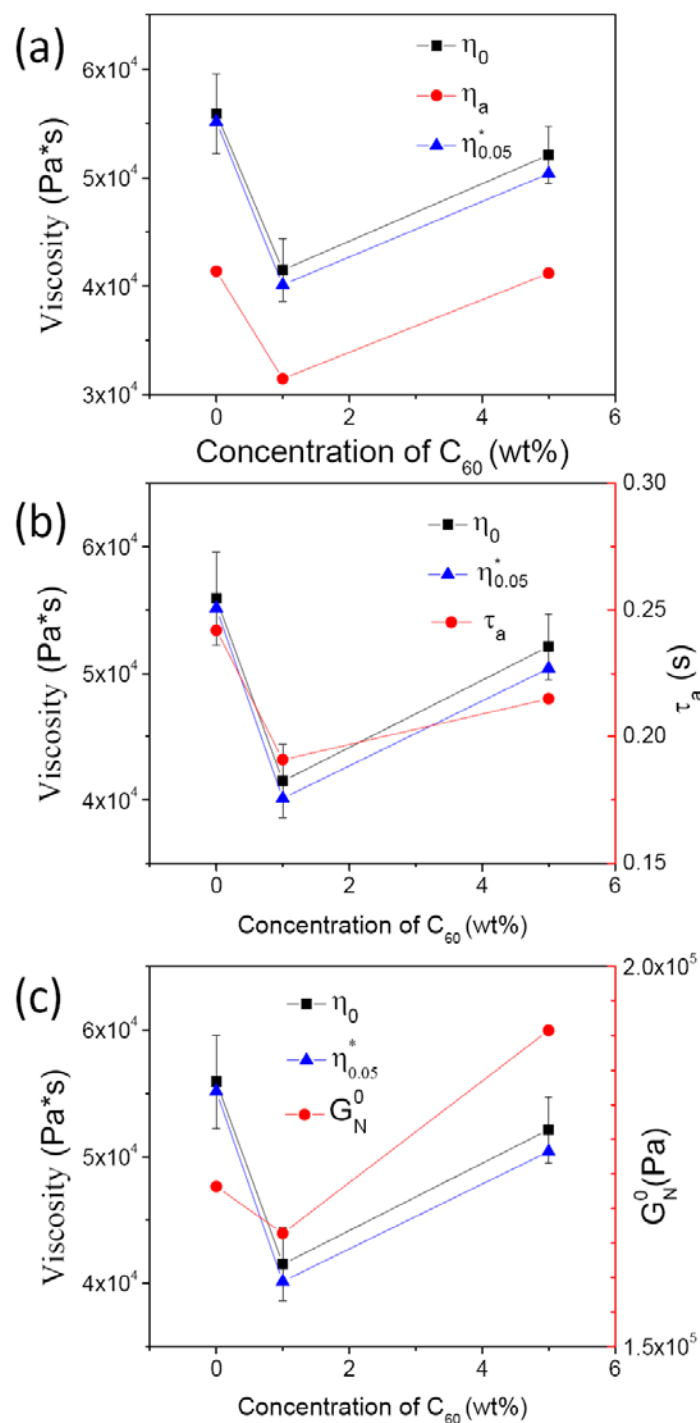


Figure S12. (a) Zero shear viscosity (η_0), complex viscosity at 0.05 rad/s ($\eta_{0.05}^*$) and apparent viscosity ($\eta_a = G_N^0 \cdot \tau_a$) of S3PS-75k/C₆₀ composites versus the concentration of C₆₀; (b) η_0 , $\eta_{0.05}^*$ and apparent relaxation time (τ_a) of S3PS-75k/C₆₀ composites versus the concentration of C₆₀; (c) η_0 , $\eta_{0.05}^*$ and plateau modulus (G_N^0) of S3PS-75k/C₆₀ composites versus the concentration of C₆₀ (Testing temperature: 150 °C).

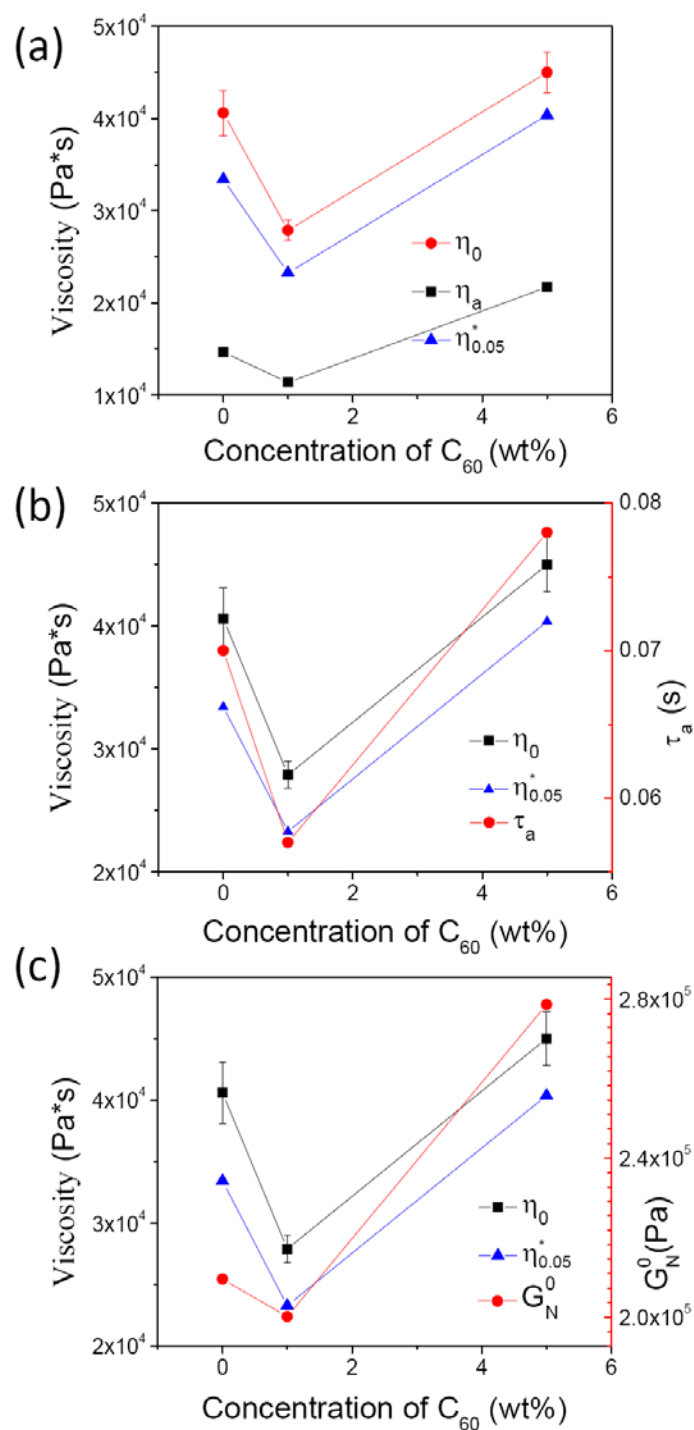


Figure S13. (a) Zero shear viscosity (η_0), complex viscosity at 0.05 rad/s ($\eta_{0.05}^*$) and apparent viscosity ($\eta_a = G_N^0 \cdot \tau_a$) of S6PS-93k/C₆₀ composites versus the concentration of C₆₀; (b) η_0 , $\eta_{0.05}^*$ and apparent relaxation time (τ_a) of S6PS-93k/C₆₀ composites versus the concentration of C₆₀; (c) η_0 , $\eta_{0.05}^*$ and plateau modulus (G_N^0) of S6PS-93k/C₆₀ composites versus the concentration of C₆₀ (Testing temperature: 150 °C).

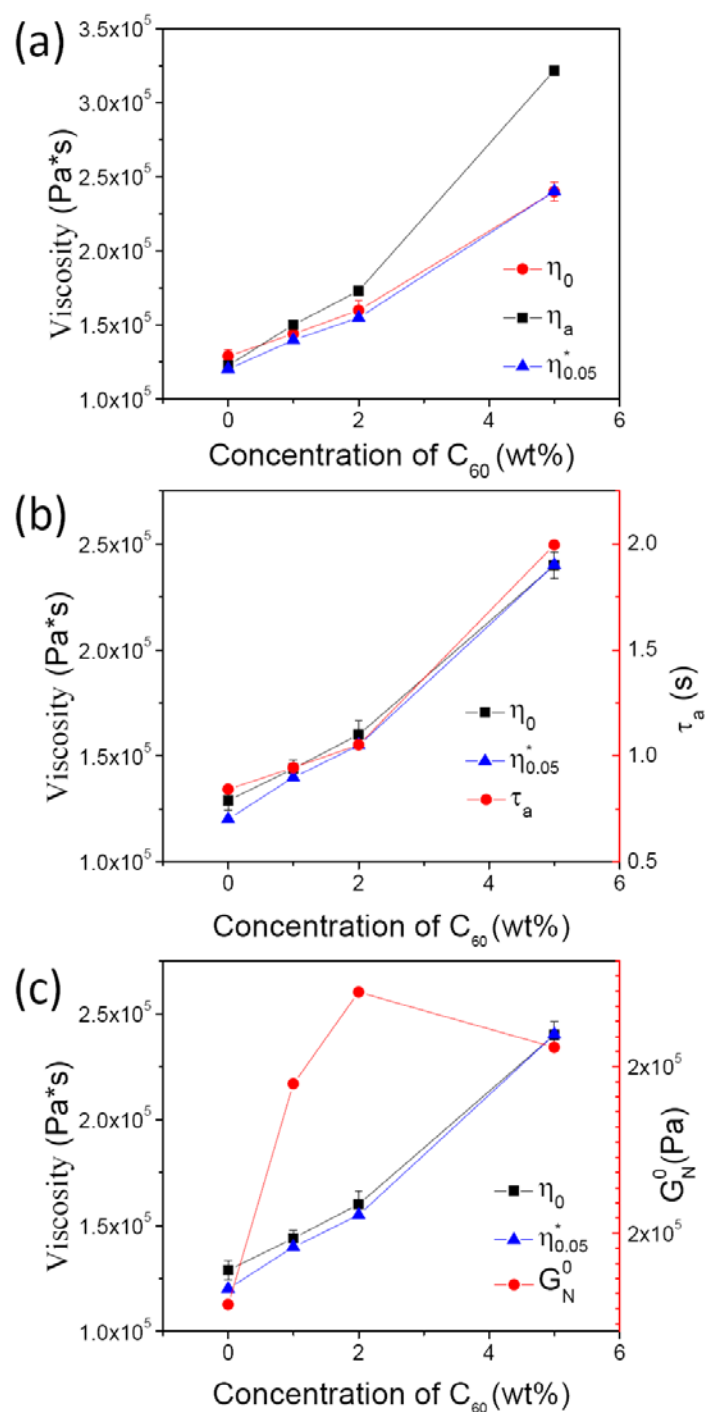


Figure S14. (a) Zero shear viscosity (η_0), complex viscosity at 0.05 rad/s ($\eta_{0.05}^*$) and apparent viscosity ($\eta_a = G_N^0 \cdot \tau_a$) of S3PS-119k/C₆₀ composites versus the concentration of C₆₀; (b) η_0 , $\eta_{0.05}^*$ and apparent relaxation time (τ_a) of S3PS-119k/C₆₀ composites versus the concentration of C₆₀; (c) η_0 , $\eta_{0.05}^*$ and plateau modulus (G_N^0) of S3PS-119k/C₆₀ composites versus the concentration of C₆₀ (Testing temperature: 150 °C).

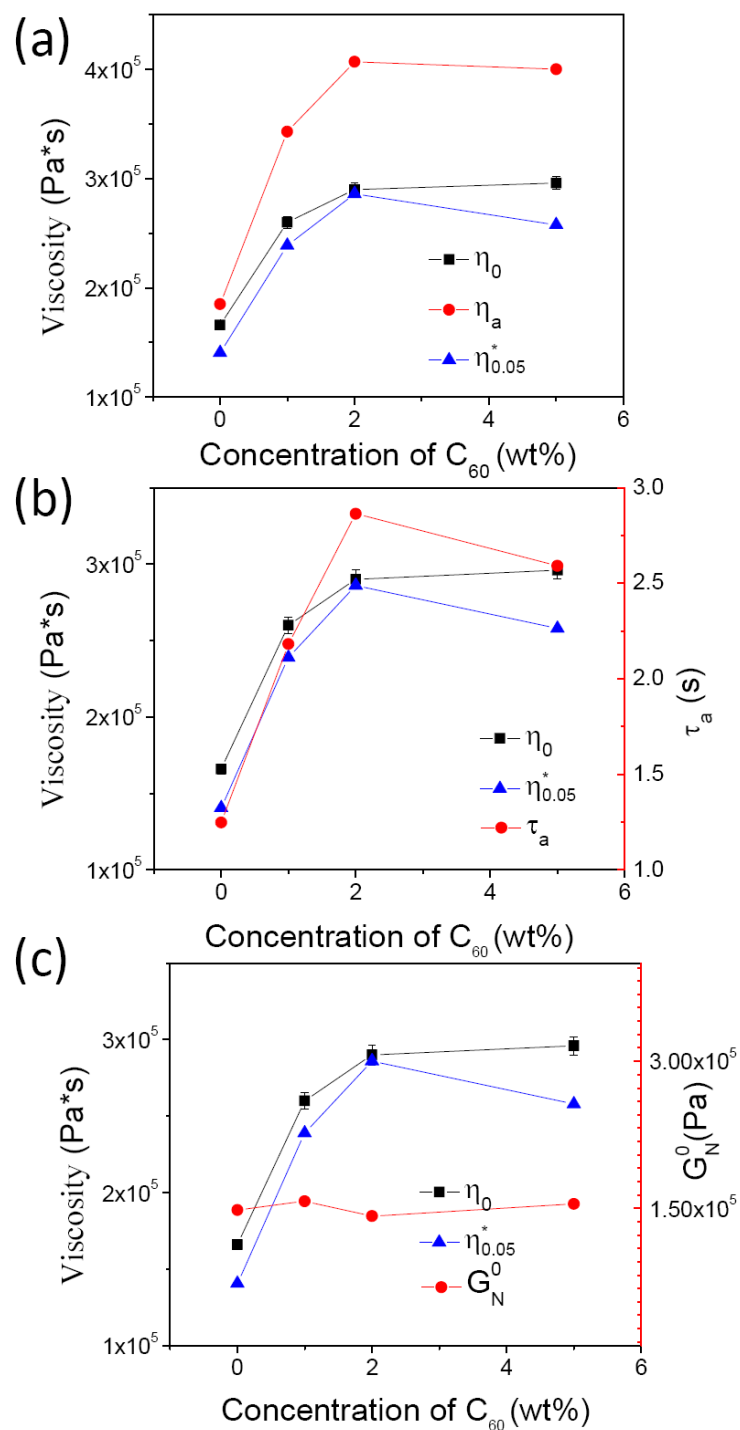


Figure S15. (a) Zero shear viscosity (η_0), complex viscosity at 0.05 rad/s ($\eta_{0.05}^*$) and apparent viscosity ($\eta_a = G_N^0 \cdot \tau_a$) of S3PS-150k/C₆₀ composites versus the concentration of C₆₀; (b) η_0 , $\eta_{0.05}^*$ and apparent relaxation time (τ_a) of S3PS-150k/C₆₀ composites versus the concentration of C₆₀; (c) η_0 , $\eta_{0.05}^*$ and plateau modulus (G_N^0) of S3PS-150k/C₆₀ composites versus the concentration of C₆₀ (Testing temperature: 150 °C).

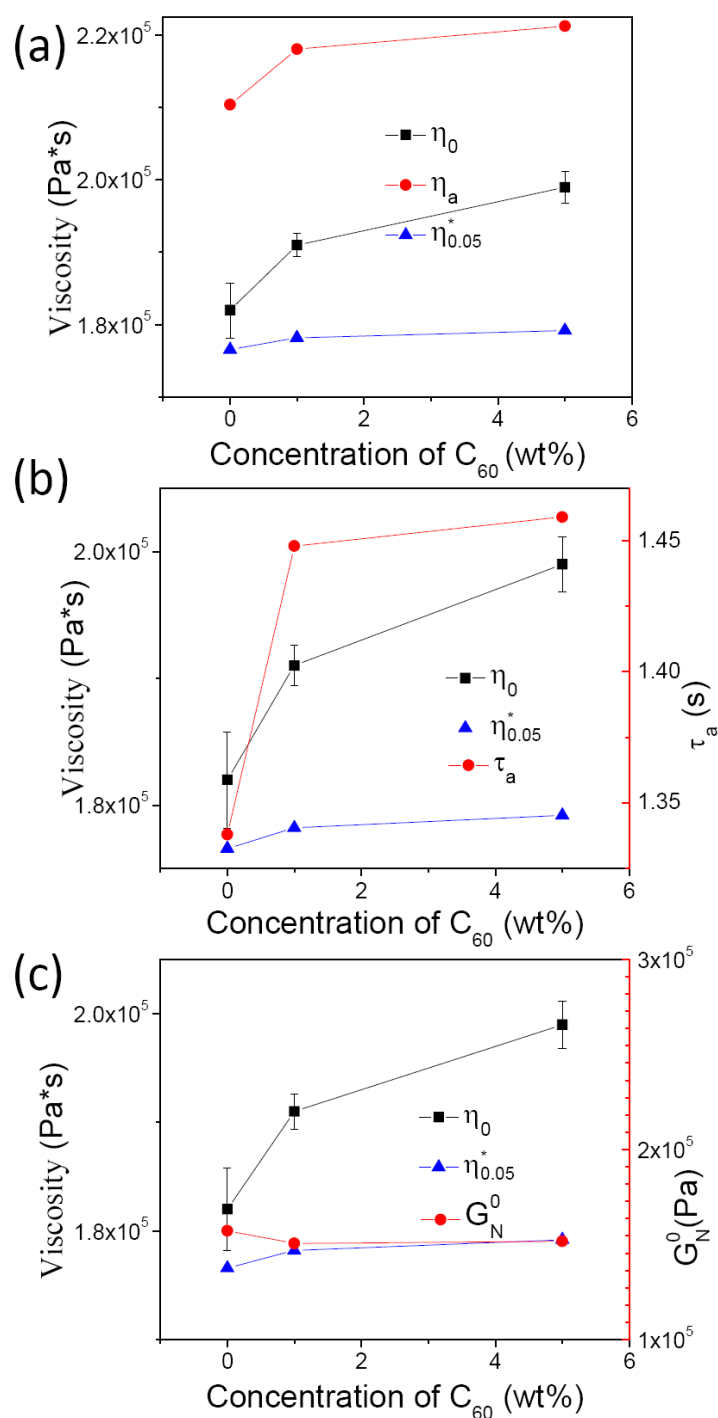


Figure S16. (a) Zero shear viscosity (η_0), complex viscosity at 0.05 rad/s ($\eta_{0.05}^*$) and apparent viscosity ($\eta_a = G_N^0 \cdot \tau_a$) of S6PS-226k/C₆₀ composites versus the concentration of C₆₀; (b) η_0 , $\eta_{0.05}^*$ and apparent relaxation time (τ_a) of S6PS-226k/C₆₀ composites versus the concentration of C₆₀; (c) η_0 , $\eta_{0.05}^*$ and plateau modulus (G_N^0) of S6PS-226k/C₆₀ composites versus the concentration of C₆₀ (Testing temperature: 150 °C).

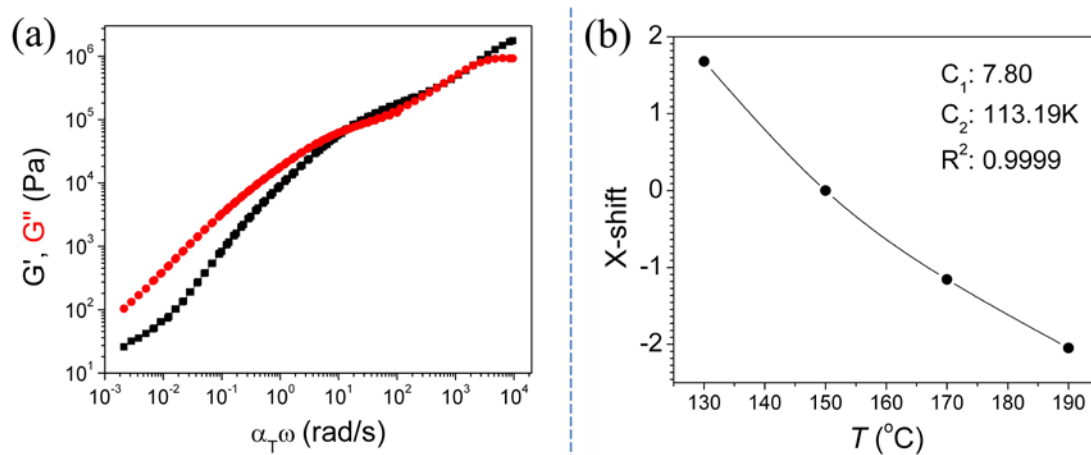


Figure 17. (a) Storage modulus (G') and loss modulus (G'') versus frequency at 150 °C. (b) Shift factor versus temperature and the calculated C_1 and C_2 values at 150 °C.

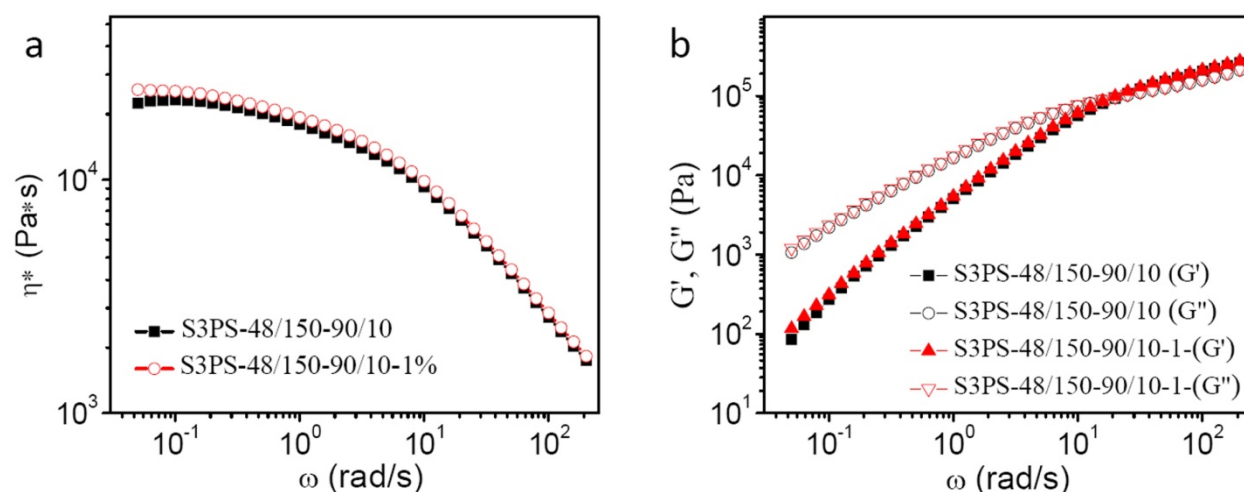


Figure S18. Complex viscosity (η^*), storage (G') and loss (G'') moduli versus frequency (ω) for S3PS-48k/S3PS-150k blend with 1 wt% C_{60} . Weight fraction of S3PS-150k was 10%.

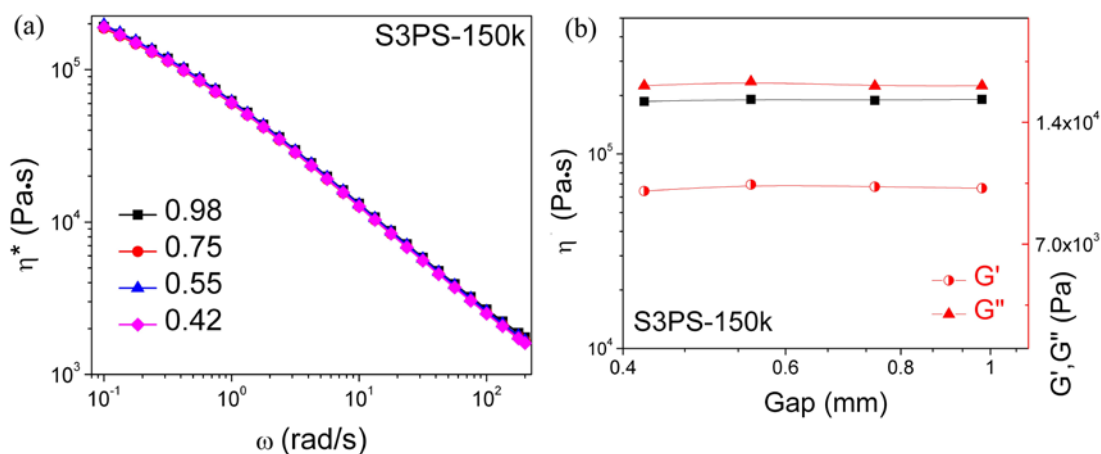


Figure R19. (a) Complex viscosity versus frequency at different gaps at 150 °C; (b) Comparison of complex viscosity, storage modulus and loss modulus versus gaps at 0.1 rad/s at 150 °C.

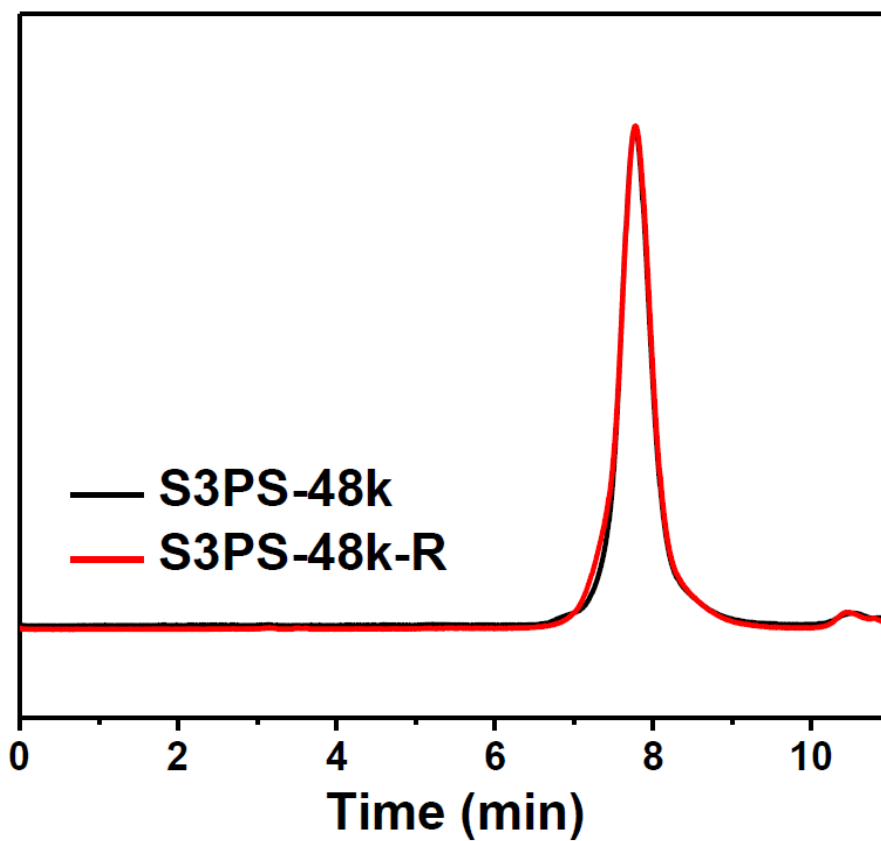


Figure S20. Elution curves of S3PS-48k from SEC measurement. The symbol ‘R’ represents the sample suffering rheological test.

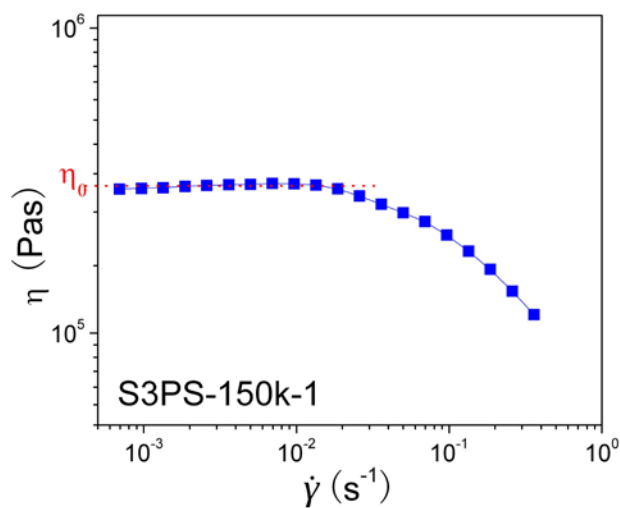


Figure S21. Steady-state viscosities for S3PS-150k-1 at 150 °C as an example to show how the zero shear viscosity (η_0) was determined.